IEEE Transactions on Aerospace and Electronic Systems,
Volume 58, Issue 5, October 2022, pp. 4782-4795
DOI:10.1109/TAES.2022.3160990

Unified Control Parameterization Approach for Finite-Horizon Feedback Control with Trajectory Shaping

Namhoon Cho, *Member, IEEE,* Jongho Park,
Youdan Kim, *Senior Member, IEEE,* and Hyo-Sang Shin

Abstract

This study presents control parametrisation as a unifying framework for designing a linear feedback control law that achieves finite-time transfer of output as well as trajectory shaping. Representing control input as a linear combination of independent basis functions allows wide variability in the resultant feedback control laws through selection of the number and types of basis functions. Given an array of basis functions that meets the trajectory shaping necessities, the unified design approach proceeds with determination of the coefficients so that the predicted trajectory attains the desired output at the final time. The input evaluated with the coefficients found at each instance essentially turns out to be a linear state feedback policy with an additional feedforward term and time-dependent gains which is appropriate for practical use. The unified control parametrisation approach lends itself well to missile guidance applications with the expandability and direct trajectory shaping capability that it provides. To emphasise expandability of the framework, this study revisits the trajectory shaping guidance laws from the control parametrisation viewpoint and shows how the notion of specifying input basis functions not only generalises various existing methods but also enables further extensions. Furthermore, an application to integrated guidance and control illustrates the strength of design process in handling the shaping requirements more directly through construction of appropriate basis.

Index Terms

Terminal Control, Control Parametrisation, Basis Function, Missile Guidance, Trajectory Shaping

This work was supported by the National Research Foundation of Korea (NRF) grant funded by the Korean government (MSIT) (No. 2021R1G1A1003429).

Namhoon Cho is with the Centre for Autonomous and Cyber-Physical Systems, Cranfield University, Cranfield, Bedfordshire, MK43 0AL, United Kingdom. e-mail: n.cho@cranfield.ac.uk

Jongho Park is with the Department of Military Digital Convergence, Department of AI Convergence Network, Ajou University, Suwon, Gyeonggi-do, 16499, Republic of Korea. e-mail: parkjo05@ajou.ac.kr

Youdan Kim is with the Department of Aerospace Engineering, Institute of Advanced Aerospace Technology, Seoul National University, Seoul, 08826, Republic of Korea. e-mail: ydkim@snu.ac.kr

Hyo-Sang Shin is with the Centre for Autonomous and Cyber-Physical Systems, Cranfield University, Cranfield, Bedfordshire, MK43 0AL, United Kingdom. e-mail: h.shin@cranfield.ac.uk

© 2022 IEEE. Personal use of this material is permitted. Permission from IEEE must be obtained for all other uses, in any current or future media, including reprinting/republishing this material for advertising or promotional purposes, creating new collective works, for resale or redistribution to servers or lists, or reuse of any copyrighted component of this work in other works

I. Introduction

Various application areas involving autonomous systems such as aerospace vehicles require a controller that brings the system output to a desired final value in finite time. The problem class that considers final output boundary condition as a hard constraint has importance in systems highly concerning the achieved accuracy. Optimal control theory provides a systematic way to solve the constrained finite-horizon control problems. Formulations that can be brought to Linear Quadratic Regulator (LQR) problems are particularly useful because the solutions can be obtained in feedback form [1]–[3]. Control laws for terminal control purpose inherently have explicit time-dependence.

Although the finite-horizon LQR approach is successful and theoretically sound, its design process involves several difficulties in implementations to systems with many state variables. One arises from backward numerical solution of the associated matrix differential Riccati equation. Explicit integration is prone to computational instability and inefficiency. Modern convex programming algorithms are able to solve the problem efficiently without invoking the differential Riccati equation [4], [5]. However, the convex optimisation approaches typically entail low-order time-discretisation of the system dynamics into an affine equality constraint [6], [7], which inevitably results in some approximation errors. Also, the problem size increases with a finer choice of discretisation step size.

Another difficulty lies in the complexity of adjusting trajectories to exhibit desired characteristics through tuning of the performance index weightings. The shaping requirements of a given mission are usually only qualitative descriptions. However, translation into quantitative specifications in terms of LQR weightings is a difficult design choice to make. One of the reasons is that mapping from weightings to feedback gains in the LQR formalism is non-injective, i.e., many-to-one. Therefore, shaping can be done only indirectly through trials-and-errors involving different forms of weightings relying on the trend that a higher penalty on one variable will suppress its relative accumulation over time in comparison to other variables. This indirect tuning process may easily lose consistency. The situation becomes even more complicated when weightings are considered to be time-varying to allow enough flexibility.

The primary objective of this study is to present a complementary approach that enables more direct trajectory shaping in the design of controllers for finite-horizon output transfer. This study takes inspirations from control parametrisation techniques that were originally developed in the context of approximate trajectory optimisation [8]–[11]. The proposed approach begins with parametrising the control input as a linear combination of user-specified basis functions. The parametrised control solution can equivalently be regarded as a feedback policy if the coefficients are related to each initial state through a closed-form expression. This is possible in linear systems whose time-domain solution can always be described

explicitly. Noticing from these observations, the proposed control parametrisation approach obtains control laws in *feedback* form by satisfying the targeted final output condition with the closed-loop trajectory predicted at each instance.

This study highlights the utility of the unified control parametrisation approach in missile trajectory shaping guidance. Especially, it will be shown that appropriate design of input basis functions enables the capability of more direct trajectory shaping and expandability. As the first step, this study provides a unifying viewpoint for design of guidance laws. Control parametrisation is shown to be an alternative framework that can produce various guidance laws based on LQR as special cases by taking different types of basis functions. Then, this study introduces a more detailed application to integrated guidance and control synthesis illustrating the constructive design process based on building basis functions as needed. These examples show that the unified control parametrisation approach not only encompasses existing methods, but also enables design of new ones effective in specific applications.

This study focuses on providing a holistic overview of the control parametrisation approach and its utility in guidance systems for tactical missiles. Notable contributing points are summarised below:

- (Optimality Relation for Control Parametrisation Method) An explicit relation between the input basis functions and the LQR weighting functions is derived to show how the control parametrisation approach is connected to optimal control.
- (Analysis of Existing Guidance Laws) Inclusion relationship between various existing guidance laws is thoroughly articulated in terms of input basis functions not only to revisit previous studies but also to enable further generalisation. This will allow developments of new guidance laws that could not be derived using existing guidance laws.
- (Integrated Guidance and Control Application) The concept of control activation function and its usefulness in the composition of input basis functions is presented and demonstrated with an integrated guidance and control design example.

This paper proceeds as follows: Section II discusses the design methodology based on control parametrisation. Subsequent sections illustrate the characteristics of this basis-oriented design approach applied to missile guidance. Section III establishes a unified understanding about the trajectory shaping guidance laws focused on identifying associated basis functions, on the line extending [12]. Section IV presents a numerical example showcasing the design process and effects of basis functions in integrated guidance and control for homing in the vertical plane. Concluding remarks are given in Sec. V.

II. Control Parametrisation Approach to Terminal Control Problem

This section formally describes a control design method based on specifying certain parametrisation for the control input to solve a class of finite-horizon control problems with terminal output constraint. The coefficient determination procedures are detailed for two possible cases distinguished by the difference in the number of terminal constraints and basis functions.

A. Problem Formulation

Consider a linear time-varying system with additional forcing term

$$\begin{aligned} \dot{\mathbf{x}}(t) &= \mathbf{A}(t)\mathbf{x}(t) + \mathbf{B}(t)\mathbf{u}(t) + \mathbf{c}(t) \\ \mathbf{z}(t) &= \mathbf{E}\mathbf{x}(t) \end{aligned} \tag{1}$$

where $\mathbf{x}(t) \in \mathbb{R}^{n\times 1}$ represents the state, $\mathbf{u}(t) \in \mathbb{R}^{m\times 1}$ denotes the input, $\mathbf{z}(t) \in \mathbb{R}^{p\times 1}$ refers to the performance output. $(\mathbf{A}(t), \mathbf{B}(t), \mathbf{c}(t))$ are known matrices, $\mathbf{E} \in \mathbb{R}^{p\times n}$ is a known constant matrix with $\operatorname{rank}(\mathbf{E}) = p \leq n$, and the notation $\dot{()}$ represents differentiation with respect to t. Note that the independent variable t is not confined only to represent time, rather it can be other quantities having monotonic relationship with respect to time. The pair $(\mathbf{A}(t), \mathbf{B}(t))$ is assumed to be controllable.

This study concerns a class of terminal control problems to design a control input $\mathbf{u}(t)$ so that the state evolved according to Eq. (1) satisfies

$$\mathbf{E}\mathbf{x}(t_f) = \mathbf{z}_{f_d} \tag{2}$$

at the fixed final time t_f where $\mathbf{z}_{f_d} \in \mathbb{R}^{p\times 1}$ is a known constant vector. The assumption on $\mathbf{E}$ being full (row) rank means that the affine equality constraints are mutually independent and their number is less than or equal to the dimension of state.

Linear time-varying systems frequently arise from finite-horizon trajectory tracking problems. Given a nominal trajectory consisting of time profiles for state and input $\{\mathbf{x}_0(t), \mathbf{u}_0(t)\}$, a nonlinear dynamic system $\dot{\mathbf{x}}(t) = \mathbf{f}(\mathbf{x}(t), \mathbf{u}(t))$ can be linearised at the nominal trajectory. Then, the perturbed system $\dot{\bar{\mathbf{x}}} = \partial_{\mathbf{x}}\mathbf{f}|_{\mathbf{x}_0,\mathbf{u}_0}\,\bar{\mathbf{x}} + \partial_{\mathbf{u}}\mathbf{f}|_{\mathbf{x}_0,\mathbf{u}_0}\,\bar{\mathbf{u}}$ with $\bar{\mathbf{x}} \triangleq \mathbf{x} - \mathbf{x}_0$ and $\bar{\mathbf{u}} \triangleq \mathbf{u} - \mathbf{u}_0$ is linear time-varying since the Jacobians evaluated along the nominal trajectory are time-dependent.

B. Control Parametrisation

The proposed approach leverages a structured parametrisation for the input given by

$$\mathbf{u}(t) = \mathbf{\Psi}^T(t)\,\mathbf{k} \tag{3}$$

where $\mathbf{\Psi}(t) \in \mathbb{R}^{q\times m}$ is a basis function matrix and $\mathbf{k} \in \mathbb{R}^{q\times 1}$ is a constant coefficient vector. It is worth emphasising here that the basis functions depend only on t. The proposed approach proceeds in two consecutive steps; i) choice of the number q and types of the functions constituting $\mathbf{\Psi}(t)$, and ii) determination of $\mathbf{k}$ to satisfy the equality constraints in Eq. (2).

The control parametrisation approach offers great variability in design through the freedom in choosing $\mathbf{\Psi}(t)$. First, the number of basis functions is one of the design choices. $q = p$ is the minimal number required for existence of solution satisfying the terminal constraint. Setting $q > p$ yields more flexibility in shaping to allow for other considerations besides constraint satisfaction. Depending on whether the number of basis functions matches or exceeds that of equality constraints, Sec. II-C and Sec. II-D consider the cases of exact-parametrisation and over-parametrisation, respectively. Also, choosing different types of basis functions results in different solution behaviour. For example, the final input $\mathbf{u}(t_f)$, the final input rate $\dot{\mathbf{u}}(t_f)$, and higher derivatives will be zero regardless of the initial condition, if the basis functions and their time derivatives vanish at t_f. Or, state evolution in alternating directions can be induced for better estimation purpose by using the basis functions changing their sign during operation. Lastly, the input basis function determines the convergence properties of the closed-loop system such as the rate of convergence in output tracking error and the region of attraction. Therefore, the desired convergence characteristics is an important consideration for the choice of appropriate basis function.

The solution for the linear system of Eq. (1) initiating from the current time t can be expressed as

$$\mathbf{x}(\tau) = \mathbf{\Phi}(\tau, t)\,\mathbf{x}(t) + \int_t^\tau \mathbf{\Phi}(\tau, \eta)\left\{\mathbf{B}(\eta)\,\mathbf{u}(\eta) + \mathbf{c}(\eta)\right\} d\eta \tag{4}$$

where $\tau > t$ is a future time and $\mathbf{\Phi}(t_2, t_1)$ denotes the state transition matrix from t_1 to t_2 which satisfies $\frac{d\mathbf{\Phi}(t,t_0)}{dt} = \mathbf{A}(t)\,\mathbf{\Phi}(t, t_0)$ and $\mathbf{\Phi}(t_0, t_0) = \mathbf{I}$, $\forall t_0$. By substituting Eq. (3) into Eq. (4), the state resulting from the linearly parametrised control can be rewritten as

$$\mathbf{x}(\tau) = \mathbf{F}(\tau, t)\,\mathbf{k} + \mathbf{\Phi}(\tau, t)\,\mathbf{x}(t) + \mathbf{f}(\tau, t) \tag{5}$$

where

$$\begin{aligned} \mathbf{F}(\tau, t) &\triangleq \int_t^\tau \mathbf{\Phi}(\tau, \eta)\,\mathbf{B}(\eta)\,\mathbf{\Psi}^T(\eta)\,d\eta \\ \mathbf{f}(\tau, t) &\triangleq \int_t^\tau \mathbf{\Phi}(\tau, \eta)\,\mathbf{c}(\eta)\,d\eta \end{aligned} \tag{6}$$

It is noticeable from Eqs. (5) and (6) that the state solution is linear in both coefficient $\mathbf{k}$ and the current state $\mathbf{x}(t)$.

We will assume that the basis function matrix is chosen appropriately considering the trajectory design requirements. The next step in the design procedure is coefficient determination.

C. Determined Case

Let us suppose that $\dim(\mathbf{k}) = \dim(\mathbf{z}_{f_d})$, i.e., $q = p$. Assuming that the system dynamics is not corrupted by any uncertainties, the final state can be predicted by evaluating the state solution in Eq. (5) at t_f, i.e.,

$$\mathbf{x}(t_f) = \mathbf{F}(t_f, t)\,\mathbf{k} + \mathbf{\Phi}(t_f, t)\,\mathbf{x}(t) + \mathbf{f}(t_f, t) \tag{7}$$

Substituting Eq. (7) into Eq. (2) and rewriting the result about the coefficient vector yields

$$\mathbf{EF}(t_f, t)\,\mathbf{k} = \mathbf{z}_{f_d} - \mathbf{E\Phi}(t_f, t)\,\mathbf{x}(t) - \mathbf{Ef}(t_f, t) \tag{8}$$

Here, $\mathbf{EF}(t_f, t)$ is a square matrix. Equation (8) shows that coefficient determination reduces to solving a fully-determined system of linear equations. If $\mathbf{EF}(t_f, t)$ is nonsingular, there exists a unique solution. Otherwise, if Eq. (8) is consistent and $\mathbf{EF}(t_f, t)$ is rank-deficient, the set of linear equations has an infinitude of solutions. In this case, the Moore-Penrose pseudoinverse can be used to construct the unique minimum-norm solution. The solution can be written in either cases as

$$\mathbf{k} = \{\mathbf{EF}(t_f, t)\}^{\dagger}\{\mathbf{z}_{f_d} - \mathbf{E\Phi}(t_f, t)\,\mathbf{x}(t) - \mathbf{Ef}(t_f, t)\} \tag{9}$$

where $()^{\dagger}$ denotes the pseudoinverse. The coefficient vector is treated as a constant and solved for *each* current time t to satisfy the equality constraints at a moment t_f with the *instantaneous predicted* trajectory. Readers are referred to Appendix A for the invariance of $\mathbf{k}$ along the ideal trajectory.

Finally, the control law can be obtained by substituting Eq. (9) into Eq. (3) as

$$\mathbf{u}(t) = -\mathbf{K}_1(t)\,\mathbf{x}(t) + \mathbf{v}_1(t) \tag{10}$$

where

$$\begin{aligned} \mathbf{K}_1(t) &\triangleq \mathbf{\Psi}^T(t)\{\mathbf{EF}(t_f, t)\}^{\dagger}\mathbf{E\Phi}(t_f, t) \\ \mathbf{v}_1(t) &\triangleq \mathbf{\Psi}^T(t)\{\mathbf{EF}(t_f, t)\}^{\dagger}\{\mathbf{z}_{f_d} - \mathbf{Ef}(t_f, t)\} \end{aligned} \tag{11}$$

Equation (10) clearly shows that the proposed approach results in a linear state feedback control law including an additional feedforward term with time-varying gains.

Remark 1 (Relation Between Basis Function in Control Parametrisation and Weighting Function in Linear Quadratic Regulator)**.**

The relation between input basis functions and the corresponding cost function being minimised can provide useful insights aiding choice of basis functions. Full characterisation of inverse optimality can be performed by solving the associated inverse linear quadratic optimal control problem [13]. However, the general solution is not unique because the map from combination of weightings to the optimal feedback gain is many-to-one. An obvious particular solution can be obtained by directly comparing the feedback

gain given in Eq. (11) and that for a LQR with no state weightings. It is well-known that the solution minimising the weighted control effort given by

$$J = \int_t^{t_f} \mathbf{u}^T(\tau)\,\mathbf{R}(\tau)\,\mathbf{u}(\tau)\,d\tau \tag{12}$$

with $\mathbf{R}(\tau) = \mathbf{R}^T(\tau) > 0$ subject to Eqs. (1) and (2) is obtained as

$$\mathbf{u}^*(t) = -\mathbf{K}^*(t)\,\mathbf{x}(t) + \mathbf{v}^*(t) \tag{13}$$

where

$$\begin{aligned}
\mathbf{K}^*(t) &= \mathbf{R}^{-1}(t)\,\mathbf{B}^T(t)\,\mathbf{\Phi}^T(t_f,t)\,\mathbf{E}^T\left\{\mathbf{E}\int_t^{t_f}\mathbf{\Phi}(t_f,\tau)\,\mathbf{B}(\tau)\,\mathbf{R}^{-1}(\tau)\,\mathbf{B}^T(\tau)\,\mathbf{\Phi}^T(t_f,\tau)\,d\tau\mathbf{E}^T\right\}^{-1}\mathbf{E}\mathbf{\Phi}(t_f,t)\\
\mathbf{v}^*(t) &= \mathbf{R}^{-1}(t)\,\mathbf{B}^T(t)\,\mathbf{\Phi}^T(t_f,t)\,\mathbf{E}^T\left\{\mathbf{E}\int_t^{t_f}\mathbf{\Phi}(t_f,\tau)\,\mathbf{B}(\tau)\,\mathbf{R}^{-1}(\tau)\,\mathbf{B}^T(\tau)\,\mathbf{\Phi}^T(t_f,\tau)\,d\tau\mathbf{E}^T\right\}^{-1}\left(\mathbf{z}_{f_d}-\mathbf{E}\int_t^{t_f}\mathbf{\Phi}(t_f,\tau)\,\mathbf{c}(\tau)\,d\tau\right)
\end{aligned} \tag{14}$$

Comparison of Eqs. (11) and (14) shows that a control parametrisation design becomes identical to the minimum effort solution if the basis function $\mathbf{\Psi}(t)$ is related to the weighting function $\mathbf{R}(t)$ through

$$\mathbf{\Psi}(t) = \mathbf{E}\mathbf{\Phi}(t_f,t)\,\mathbf{B}(t)\,\mathbf{R}^{-1}(t) \tag{15}$$

D. Underdetermined Case

This section addresses the case where $\dim(\mathbf{k}) > \dim(\mathbf{z}_{f_d})$, i.e., $q > p$, thus the system of equations is underdetermined. The solution is not unique as there remain $\dim(\mathbf{k}) - \dim(\mathbf{z}_{f_d})$ degrees-of-freedom after taking into account the equality constraints.

One reasonable approach to fully determine the coefficient is to solve an optimisation problem

$$\begin{aligned}
&\text{minimise} && J = \frac{1}{2}\mathbf{x}^T(t_f)\mathbf{W}\mathbf{x}(t_f) + \frac{1}{2}\int_t^{t_f}\left[\mathbf{x}^T(\tau)\,\mathbf{Q}(\tau)\,\mathbf{x}(\tau) + \mathbf{u}^T(\tau)\,\mathbf{R}(\tau)\,\mathbf{u}(\tau)\right]d\tau\\
&\text{subject to} && \mathbf{E}\mathbf{x}(t_f) = \mathbf{z}_{f_d}
\end{aligned} \tag{16}$$

where $\mathbf{W} = \mathbf{W}^T > 0$, $\mathbf{Q}(t) = \mathbf{Q}^T(t) \geq 0$, and $\mathbf{R}(t) = \mathbf{R}^T(t) > 0$. The design objective of this formulation is finite-horizon regulation which requires i) transfer of performance output to the desired final value ii) while keeping other state and input variables small. The above optimisation problem applies to every instance considering the current time t as the given initial point for predicting the state solution.

By substituting Eqs. (3)-(5), the problem in Eq. (16) can be represented as the following Quadratic Programming (QP) problem with $\mathbf{k}$ as the decision variable.

$$\begin{aligned}
&\text{minimise} && J = \frac{1}{2}\mathbf{k}^T\mathbf{G}(t)\,\mathbf{k} + \mathbf{g}^T(t)\,\mathbf{k}\\
&\text{subject to} && \mathbf{E}\mathbf{F}(t_f,t)\,\mathbf{k} = \mathbf{z}_{f_d} - \mathbf{E}\mathbf{\Phi}(t_f,t)\,\mathbf{x}(t) - \mathbf{E}\mathbf{f}(t_f,t)
\end{aligned} \tag{17}$$

where

$$\begin{aligned}
\mathbf{G}(t) &\triangleq \mathbf{F}^T(t_f,t)\,\mathbf{W}\mathbf{F}(t_f,t) + \int_t^{t_f}\left[\mathbf{F}^T(\tau,t)\,\mathbf{Q}(\tau)\,\mathbf{F}(\tau,t) + \mathbf{\Psi}(\tau)\,\mathbf{R}(\tau)\,\mathbf{\Psi}^T(\tau)\right]d\tau\\
\mathbf{g}(t) &\triangleq \mathbf{F}^T(t_f,t)\,\mathbf{W}\left\{\mathbf{\Phi}(t_f,t)\,\mathbf{x}(t) + \mathbf{f}(t_f,t)\right\} + \int_t^{t_f}\mathbf{F}^T(\tau,t)\,\mathbf{Q}(\tau)\left\{\mathbf{\Phi}(\tau,t)\,\mathbf{x}(t) + \mathbf{f}(\tau,t)\right\}d\tau
\end{aligned} \tag{18}$$

The control law can be obtained by substituting the optimal solution of Eq. (17) into Eq. (3) as

$$\mathbf{u}(t) = -\mathbf{K}_2(t)\,\mathbf{x}(t) + \mathbf{v}_2(t) \tag{19}$$

where

$$\begin{aligned}
\mathbf{K}_2(t) &\triangleq \boldsymbol{\Psi}^T(t)\,\mathbf{G}^{-1}(t)\,\{\mathbf{EF}(t_f,t)\}^T\left[\mathbf{EF}(t_f,t)\,\mathbf{G}^{-1}(t)\,\{\mathbf{EF}(t_f,t)\}^T\right]^{-1}\mathbf{E}\boldsymbol{\Phi}(t_f,t)\\
\mathbf{v}_2(t) &\triangleq \boldsymbol{\Psi}^T(t)\,\mathbf{G}^{-1}(t)\left[\{\mathbf{EF}(t_f,t)\}^T\left[\mathbf{EF}(t_f,t)\,\mathbf{G}^{-1}(t)\,\{\mathbf{EF}(t_f,t)\}^T\right]^{-1}\left\{\mathbf{EF}(t_f,t)\,\mathbf{G}^{-1}(t)\,\mathbf{g}(t)+\mathbf{z}_{f_d}-\mathbf{Ef}(t_f,t)\right\}-\mathbf{g}(t)\right]
\end{aligned} \tag{20}$$

Readers are referred to Appendix B for further details about solving the QP problem.

Remark 2. The idea of using a linearly parametrised input was presented in [14] in the context of *explicit* guidance for spacecraft. This study complements [14] with a broader scope considering generic linear time-varying systems, placing emphasis on the trajectory shaping avaiable through basis function families other than polynomials, and addressing the connection to the LQR as described in Remark 1.

III. Trajectory Shaping Guidance Laws

Expandability and direct trajectory shaping capability provided by the control parametrisation approach are well-suited for missile guidance applications. In the present context, expandability refers to the capability of the design framework for generating various new control laws as well as explaining existing ones. Also, direct trajectory shaping capability refers to the possibility of drawing a desired trajectory behaviour by directly specifying the basis functions that encode the desired time-dependent pattern for the control input.

This section aims to show the generality of the approach based on specifying input basis functions in designing homing guidance laws. This section reviews various trajectory shaping guidance laws that were originally developed based on LQR formulations and delineates them as specific instances of control parametrisation framework. Unified understanding clarifies their interconnections, the knowledge which will also be useful for designing new guidance laws. This section centres upon the design equations developed for the determined case in Sec. II-C.

A. Background

Trajectory shaping guidance refers to the designs concerning not only the point constraints at the interception, but also the overall trend of state profiles. Necessity of trajectory shaping arises from various design considerations depending on the type of mission and airframe characteristics. Command can be constructed to distribute the manoeuvre demand over engagement [15], [16], to maintain control authority near the end of engagement to cope with external disturbances [17], or to reduce sensitivity to the initial heading error [18]. Other purposes include enhancement of target observability, survivability, or kill

probability, and smooth handover at the switching boundaries between waypoints or different guidance policies. Conformance to the limits on manoeuvrability and seeker's field-of-view is also necessary. Studies on guidance laws have shown gradual advances towards sophistication by incorporating more complicated objectives as well as constraints as missile systems and missions develop.

An expandable framework is desirable to facilitate systematic and possibly automated design of guidance laws. It is because a formal method bearing rich degrees-of-freedom can find a good solution by modifying only the tunable elements. One interesting observation is that many existing trajectory shaping guidance laws commonly have the linear-in-parameter structure. This is a natural consequence of employing a linear state feedback control law.

B. Formulation

The common elements of trajectory shaping guidance design are *i) a linear system equation*, *ii) desired terminal conditions*, and *iii) parametric representation of input*. For simplicity, planar engagement of a stationary target is considered in this study. Figure 1 shows the engagement geometry and notations.

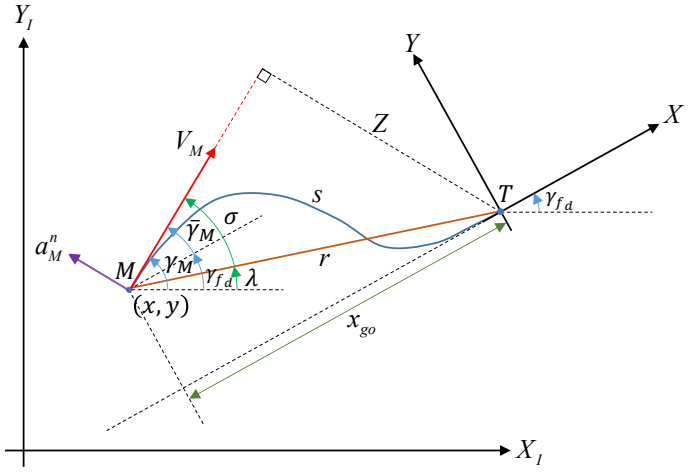

Fig. 1. Planar Engagement Geometry

In Fig. 1, (X_I, Y_I) and (X, Y) denote the inertial and the impact coordinate systems, respectively. The impact coordinate system has its origin at the stationary target denoted by T and its X-axis aligned to the desired impact direction with angle γ_{f_d} from X_I-axis. For the missile denoted by M, (x, y) is the position represented in the impact coordinate system, V_M is the speed, γ_M is the flight path angle, and a_M^n is the lateral acceleration. Also, r is the range, λ is the line-of-sight angle, σ is the lead angle, and s is the arc-length of the missile's path. The downrange-to-go denoted by x_{go} is the remaining distance to the target along X-axis, and $x_{go} = -x$ by construction. The flight path angle error is defined as follows:

$$\bar{\gamma}_M \triangleq \gamma_M - \gamma_{f_d} \tag{21}$$

The motion of the missile can be represented as

$$\begin{aligned} \dot{x} &= V_M \cos\bar{\gamma}_M, \qquad x\left(t_0\right) = x_0 \\ \dot{y} &= V_M \sin\bar{\gamma}_M, \qquad y\left(t_0\right) = y_0 \\ \dot{\bar{\gamma}}_M &= \dot{\gamma}_M = \frac{a_M^n}{V_M}, \quad \bar{\gamma}_M\left(t_0\right) = \bar{\gamma}_{M_0} = \gamma_{M_0} - \gamma_{f_d} \end{aligned} \tag{22}$$

Also, the corresponding polar coordinate representation is

$$\begin{aligned} \dot{r} &= -V_M \cos\sigma, \quad r\left(t_0\right) = r_0 \\ \dot{\lambda} &= -\frac{V_M \sin\sigma}{r}, \quad \lambda\left(t_0\right) = \lambda_0 \end{aligned} \tag{23}$$

where $\sigma \triangleq \gamma_M - \lambda$. The zero-effort-miss $Z = r\sin\sigma$ is related to the line-of-sight rate in Eq. (23) as

$$Z = -\frac{r^2}{V_M}\dot{\lambda} \tag{24}$$

1) System Equation: Many existing homing guidance laws are based on linear formulations. The system equation describing engagement kinematics is inherently nonlinear, but a linearised form has been considered in many studies by assuming small perturbation from collision course [19]. The system equation can also be obtained in linear form by change of variables [20] or by feedback linearisation [21]. Linear lowpass filter representations for the lag due to autopilot and airframe dynamics can be included in the system equation to prevent the performance degradation caused by increased contribution of autopilot lag at the end of homing [22]. A system equation of linear form is preferred to design a trajectory shaping guidance law, because the shaping can be performed with the knowledge of the closed-form solution.

Time t is the inherent independent variable of the system equation, but other variables with monotonic relation to time such as the arc-length s, the downrange x, and the range r can also serve as the independent variable. The choice of independent variable determines the form of system equation and the assumptions implicit in derivation. A noteworthy point is that the system equation will not depend on the speed V_M if a variable with physical dimension of length is taken as the independent variable and it is assumed that V_M is constant.

The variables related to the desired terminal condition are considered as the state of system equation. With regard to the requirement of interception, quantities such as the crossrange y, the zero effort miss Z, or the line-of-sight rate $\dot{\lambda}$ can be considered. To describe the impact angle constraint, the crossrange rate $\dot{y}$, the rate of zero effort miss $\dot{Z}$, or the flight path angle error $\bar{\gamma}_M$ can be the relevant state. Also, if the autopilot lag needs to be explicitly considered, the internal state variables of autopilot dynamics will be included in the overall system equation.

Which physical variable will serve as the input to the system depends upon the independent variable and system order. For example, if t is considered as the independent variable and autopilot response follows

$\dot{a}_M^n = \frac{a_{M_c}^n - a_M^n}{\tau}$, then the lateral acceleration command $a_{M_c}^n$ will be the input. Or, if x is considered as the independent variable and the vehicle is assumed to be lag-free, then the curvature $\kappa \triangleq \frac{d\gamma_M}{ds}$ serves as the input. If $\ddot{y}$ is considered as a state variable, then the jerk will be the input.

2) Terminal Output Constraint: The fundamental requirements of the missile guidance problems concern about point constraints at the final time. Nullifying zero-effort-miss is the most essential for target interception. Additional constraints may include the impact angle and terminal acceleration conditions [15], [17], [22]. The capability of controlling the impact angle can improve the attack effectiveness. Zeroing the terminal acceleration is desirable to reserve a high enough level of control authority at the end of homing. These requirements are incorporated in the fixed terminal output constraint shown in Eq. (2). Note from Eqs. (10)-(11) that the final design will contain a feedforward part if $\mathbf{z}_{f_d} \neq \mathbf{0}$ or $\mathbf{c}(t) \neq \mathbf{0}$.

3) Parametric Representation of Input: Suppose that the input can be structured as Eq. (3). Flexibility in the choice of basis functions yields expandability of design and availability of tuning. In this sense, proper construction of the basis function matrix $\mathbf{\Psi}(t)$ is the key to obtain the desired behaviour of state and input variables. Admissibility of $\mathbf{\Psi}(t)$ mainly depends on three requirements. The first is linear independence of the basis functions. Second, satisfaction of the terminal output constraint regardless of the initial condition requires invertibility of $\mathbf{EF}(t_f, t)$ in Eq. (11). Lastly, the basis functions should be bounded so as to prevent the control input from blowing up during the engagement. In summary, the set of feasible basis functions can be represented as

$$U_{\text{feas}} = \left\{ \mathbf{\Psi}(t) : [t_0, t_f] \mapsto \mathbb{R}^{p\times m} \middle| \det\left(\mathbf{EF}(t_f, t)\right) \neq 0, \mathbf{\Psi}(t) < \infty, \forall t \in [t_0, t_f] \right\} \tag{25}$$

Remark 3. To evaluate the feedback form given by Eq. (10) efficiently, the basis functions should be the ones such that the integral defining $\mathbf{F}$ in Eq. (6) admits a closed-form expression.

C. Illustrative Examples

The design procedure developed in Sec. II-C is shown to subsume many existing guidance laws. This section presents several special cases and highlights their inclusion relation focusing on the families of basis functions considered for parametric representation.

1) Pure Proportional Navigation Guidance Law: Let range r be the independent variable, and let zero effort miss Z be the state, that is, $\mathbf{x} = Z$. From Eqs. (22)-(23), we have

$$\dot{Z} = \dot{r}\sin\sigma + r\cos\sigma\dot{\sigma} = r\cos\sigma\frac{a_M^n}{V_M} \tag{26}$$

where $a_M^n = V_M\dot{\gamma}_M$. By the change of independent variable from t to r, the system equation can be expressed as

$$Z' = \frac{\dot{Z}}{\dot{r}} = -r\frac{a_M^n}{{V_M}^2} \triangleq -ru \tag{27}$$

where u is regarded as the input. Then, the corresponding system matrices can be written as

$$\mathbf{A} = 0, \quad \mathbf{B} = -r, \quad \mathbf{c} = 0, \quad \mathbf{E} = 1 \tag{28}$$

The state transition matrix is simply $\mathbf{\Phi}(r_f, r) = \exp(0) = 1$. The desired terminal condition can be written as $Z(r_f) = 0$ where $r_f = 0$.

With a function $W(r) > 0$, the basis function can be chosen as

$$\mathbf{\Psi}(r) = \frac{r}{W(r)} \tag{29}$$

The function $\mathbf{F}$ defined in Eq. (6) can be found as

$$\mathbf{F}(r_f, r) = \int_{r_f}^{r} \frac{\eta^2}{W(\eta)} d\eta \tag{30}$$

Then, using Eq. (10), the closed-loop form command can be written as

$$u(r) = -\frac{r}{W(r)} \left[\int_{r_f}^{r} \frac{\eta^2}{W(\eta)} d\eta \right]^{-1} Z(r) \tag{31}$$

Finally, rearranging Eq. (31) by considering Eqs. (27) and (24) gives the command for lateral acceleration as follows:

$$a_M^n(r) = {V_M}^2 u(r) = \frac{r^3}{W(r)} \left[\int_{r_f}^{r} \frac{\eta^2}{W(\eta)} d\eta \right]^{-1} V_M \dot{\lambda} \triangleq G(r) V_M \dot{\lambda} \tag{32}$$

The basis function in Eq. (29) can be rewritten in terms of the gain as

$$\mathbf{\Psi}(r) = \frac{KG(r)}{r^2} \exp\left(\int \frac{G(r)}{r} dr \right) \tag{33}$$

The result given in Eq. (32) is the Pure Proportional Navigation Guidance law (PPNG) with a range-varying gain $G(r)$ of which optimality is discussed in [23]. The condition required for the function $W(r)$, or equivalently $G(r)$, is also described in [23]. The Augmented Ideal Proportional Navigation Guidance law (AIPNG) for manoeuvring target interception studied in [20] is similar to PPNG in its design, and therefore, AIPNG can also be seen as an example of the control parametrisation method. Multi-phase guidance methods studied in [24]–[26] which switch the gain of PPNG from one to another in flight can be interpreted as the case with a piecewise constant $G(r)$. Since the basis function is related to the gain through Eq. (33), the gain-switching guidance laws can be regarded as special cases of the control parametrisation method, however, this view is valid only if the range at which switching occurs is perfectly known.

2) Generalised Guidance Laws for Impact Angle Control: Let time t be the independent variable, and let crossrange and its rate be the state variables, that is, $\mathbf{x} = \begin{bmatrix} y & \dot{y} \end{bmatrix}^T$. The engagement kinematics of Eq. (22) can be linearised by assuming small flight path angle error, i.e., $\bar{\gamma}_M \ll 1$, and constant speed. The linearised engagement kinematics can be described with the following system matrices

$$\mathbf{A} = \begin{bmatrix} 0 & 1 \\ 0 & 0 \end{bmatrix}, \quad \mathbf{B} = \begin{bmatrix} 0 \\ 1 \end{bmatrix}, \quad \mathbf{c} = \mathbf{0}, \quad \mathbf{E} = \mathbf{I} \tag{34}$$

for which the state transition matrix is given by

$$\mathbf{\Phi}\left(t_f, t\right) = \exp\left(\mathbf{A}\left(t_f - t\right)\right) = \begin{bmatrix} 1 & t_{go} \\ 0 & 1 \end{bmatrix} \tag{35}$$

The lateral acceleration a_M^n is the input u. The linearised model in Eq. (34) is valid in the impact coordinate system for small $\bar{\gamma}_M$. The terminal constraint representing the desired impact angle in addition to zero miss distance is written as $\mathbf{x}\left(t_f\right) = \mathbf{0}$.

Different choices of $\mathbf{\Psi}\left(t\right)$ as functions of $t_{go} \triangleq t_f - t$ result in variants, several examples of which are summarised in Table I. Note that the design parameters that appear in Table I satisfy $n > 0$ in Cases 1, 2, 3, $n > m \geq 0$ in Case 1, $\omega > 0$ in Case 3, $W\left(t\right) > 0$ in Case 4, and

$$\begin{aligned}
c_1\left(t_{go}; \omega\right) &\triangleq \left(n+1\right)\sin\left(\omega \ln t_{go}\right) - \omega\cos\left(\omega \ln t_{go}\right) \\
c_2\left(t_{go}; \omega\right) &\triangleq \left(n+1\right)\cos\left(\omega \ln t_{go}\right) + \omega\sin\left(\omega \ln t_{go}\right) \\
g_1\left(t; t_f\right) &\triangleq \int_t^{t_f} \left(t_f - \eta\right)^2 W^{-1}\left(\eta\right) d\eta \\
g_{12}\left(t; t_f\right) &\triangleq \int_t^{t_f} \left(t_f - \eta\right) W^{-1}\left(\eta\right) d\eta \\
g_2\left(t; t_f\right) &\triangleq \int_t^{t_f} W^{-1}\left(\eta\right) d\eta
\end{aligned} \tag{36}$$

Satisfying $n > m \geq 0$ in Case 1, $n > 0$ in Cases 2 and 3, and $W\left(t\right) \to \infty$ as $t \to t_f$ in Case 4 guarantees $a_M^n\left(t_f\right) = 0$.

Cases 1, 2, and 3 together complete the whole landscape of the Generalised Impact Angle Control Guidance laws (GIACG) for lag-free vehicle. The feasible region of gain coefficients and inverse optimality of the GIACG were examined in [27]. Case 1 is known as the time-to-go polynomial guidance law presented in [17] which itself includes the guidance laws minimizing control effort weighted by a power function of time-to-go derived in [15], [22], [28], [29]. Case 4 is identical to the Generalised Weighted Optimal Guidance law (GWOG) presented in [30] by minimising the weighted control effort $J = \min \int_t^{t_f} W\left(\tau\right) u^2\left(\tau\right) d\tau$. An appropriate choice of $W\left(t\right)$ should be made considering the shaping requirements. GWOG itself includes guidance laws of [15], [31], [32]. Readers are referred to [27] and [33] for performance demonstration of Cases 1-3 and Case 4, respectively.

TABLE I

GUIDANCE LAWS FOR IMPACT ANGLE CONTROL

Case	$\boldsymbol{\Psi}(t)$	$\mathbf{F}(t_f,t)$ in Eq. (6)	$\mathbf{K}_1(t)$ in Eq. (11)
1	$\begin{bmatrix} {t_{go}}^m \\ {t_{go}}^n \end{bmatrix}$	$\begin{bmatrix} \frac{1}{m+2}{t_{go}}^{m+2} & \frac{1}{n+2}{t_{go}}^{n+2} \\ \frac{1}{m+1}{t_{go}}^{m+1} & \frac{1}{n+1}{t_{go}}^{n+1} \end{bmatrix}$	$\begin{bmatrix} \frac{(m+2)(n+2)}{{t_{go}}^2} & \frac{m+n+3}{t_{go}} \end{bmatrix}$
2	${t_{go}}^n \begin{bmatrix} \ln t_{go} \\ 1 \end{bmatrix}$	$\begin{bmatrix} \frac{(n+2)\ln t_{go}-1}{(n+2)^2}t_{go} & \frac{1}{n+2}t_{go} \\ \frac{(n+1)\ln t_{go}-1}{(n+1)^2} & \frac{1}{n+1} \end{bmatrix}$	$\begin{bmatrix} \frac{(n+2)^2}{{t_{go}}^2} & \frac{2n+3}{t_{go}} \end{bmatrix}$
3	${t_{go}}^n \begin{bmatrix} \sin(\omega \ln t_{go}) \\ \cos(\omega \ln t_{go}) \end{bmatrix}$	${t_{go}}^{n+1} \begin{bmatrix} \frac{\sin(\omega \ln t_{go})+c_1(t_{go};\omega)}{(n+2)^2+\omega^2}t_{go} & \frac{\cos(\omega \ln t_{go})+c_2(t_{go};\omega)}{(n+2)^2+\omega^2}t_{go} \\ \frac{c_1(t_{go};\omega)}{(n+1)^2+\omega^2} & \frac{c_2(t_{go};\omega)}{(n+1)^2+\omega^2} \end{bmatrix}$	$\begin{bmatrix} \frac{(n+2)^2+\omega^2}{{t_{go}}^2} & \frac{2n+3}{t_{go}} \end{bmatrix}$
4	$\frac{1}{W(t)} \begin{bmatrix} t_{go} \\ 1 \end{bmatrix}$	$\begin{bmatrix} g_1(t;t_f) & g_{12}(t;t_f) \\ g_{12}(t;t_f) & g_2(t;t_f) \end{bmatrix}$	$\frac{1}{W(t)} \begin{bmatrix} \frac{g_2 t_{go}-g_{12}}{g_1 g_2-{g_{12}}^2} & \frac{g_1-2g_{12}t_{go}+g_2{t_{go}}^2}{g_1 g_2-{g_{12}}^2} \end{bmatrix}$

3) Unified Understanding of Existing Guidance Laws: The control parametrisation approach applied to the double integrator system representing point mass kinematics produces guidance laws for impact angle constrained interception. Different formulations and basis functions account for many variants. Consider the feedback gain represented as $\mathbf{K}(t) = \begin{bmatrix} \frac{k_1(t)}{{t_{go}}^2} & \frac{k_2(t)}{t_{go}} \end{bmatrix}$. The GWOG allows k_1 and k_2 to be time-varying, whereas the GIACG only allows positive constants. However, the GWOG formulation accounts for only a certain portion of the GIACG. It is because the basis function for GWOG has only single degree-of-freedom, i.e., $W(t)$, whereas the polynomial-oriented basis function for GIACG has two degrees-of-freedom, i.e., (n,m) or (n,ω). As a closing summary, a Venn diagram for the existing homing guidance laws is shown in Fig. 2. The entries in Fig. 2 are summarised in Table II.

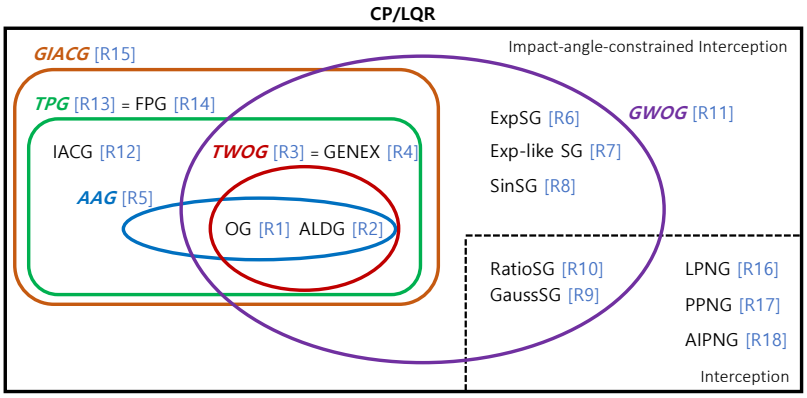

Fig. 2. Relationship Between Trajectory Shaping Guidance Laws (CP: Control Parametrisation, LQR: Linear Quadratic Regulator)

The findings suggest that new guidance laws can be derived by choosing basis functions which have not

TABLE II

TRAJECTORY SHAPING GUIDANCE LAWS FOR LAG-FREE VEHICLE MODEL

Entry	Abbreviation	Description	Reference
R1	OG	Minimum Effort Guidance	[14], [22], [34]
R2	ALDG	Apollo Lunar Descent Guidance	[35]
R3	TWOG	Time-to-Go Power Function Weighted Optimal Guidance	[15]
R4	GENEX	General Vector Explicit Guidance	[28]
R5	AAG	Augmented Apollo Powered Descent Guidance	[36]
R6	ExpSG	Exponential Function Shaping Guidance	[31]
R7	Exp-like SG	Exponential-like Function Shaping Guidance	[32]
R8	SinSG	Sinusoidal Function Shaping Guidance	[37]
R9	GaussSG	Gaussian Function Shaping Guidance	[16]
R10	RatioSG	Rational Function Shaping Guidance	[18]
R11	GWOG	Generalised Weighted Optimal Guidance	[30], [33]
R12	IACG	Interception Angle Control Guidance	[38]
R13	TPG	Time-to-Go Polynomial Guidance	[17]
R14	FPG	Fractional-Polynomial Guidance	[29]
R15	GIACG	Generalised Impact Angle Control Guidance	[27]
R16	LPNG	Linearised Proportional Navigation Guidance	[13]
R17	PPNG	Pure Proportional Navigation Guidance	[23]
R18	AIPNG	Augmented Ideal Proportional Navigation Guidance	[20]

been previously considered as long as they belong to the feasible set characterised as Eq. (25). In particular, the direction for further exploration will be to find new types of linearly independent functions lying outside the basis of the GIACG and GWOG. One such example is $\mathbf{\Psi}(t) = \begin{bmatrix} W_1(t)\, {t_{go}}^m & W_2(t)\, {t_{go}}^n \end{bmatrix}^T$ with arbitrary functions $W_1(t), W_2(t) > 0$ and constant parameters $n > m$. Moreover, another important direction for developing new guidance laws will be to overparametrise the input as done in Sec. II-D.

IV. INTEGRATED GUIDANCE AND CONTROL FOR HOMING IN VERTICAL PLANE

This section illustrates the utility of control parametrisation approach by demonstrating the actual design process with an example of integrated guidance and control for missiles. The main emphasis is on the notion of constructing the well-suited basis functions in design practices. Section IV-B describes the problem, and Sec. IV-C presents the simulation results.

A. Background

The usual approach to design a guidance and control system for a missile leverages the sequential loop-closure method considering separation between associated time scales, resulting in a cascaded structure. The autopilot is typically designed as an *infinite-horizon* tracking control law with tabulated gains indexed

by slow-varying scheduling variables, but usually not according to the mission progress measured by time-to-go. On the other hand, the guidance loop is typically designed as a *finite-horizon* regulation control law with time-varying gains approaching infinity as the engagement comes to an end. The guidance loop bandwidth increases rapidly as time-to-go converges to zero, whereas the autopilot bandwidth remains at a certain level without much change. As a result, the time-scale separation assumption becomes no longer valid as the missile approaches close to the target. The separated guidance and control design paradigm might fail to perform as expected or even lead to instability.

A remedy to overcome this difficulty is to synthesize the controller by considering the overall system dynamics that includes both engagement kinematics and airframe short-period mode dynamics. The integrated guidance and control methods have been presented in [39]–[46] based on various control synthesis schemes. Confining the scope of discussions to the linear design methods, LQR theory provides a rich formulation framework, however, a control designer might confront with the subtleties of finite-horizon LQR method [42], [45].

The control parametrisation approach renders itself viable for control synthesis in this aerospace-domain application, because trajectory shaping is necessary for reliable homing performance. It is desirable to nullify the angle of attack, the miss distance, and the impact angle error, while maintaining a sufficient level of control authority to counteract the external disturbances near the interception. Reducing the control surface deflection and its rate poses additional complications.

B. Formulation

Consider a two-dimensional homing problem in the vertical plane.

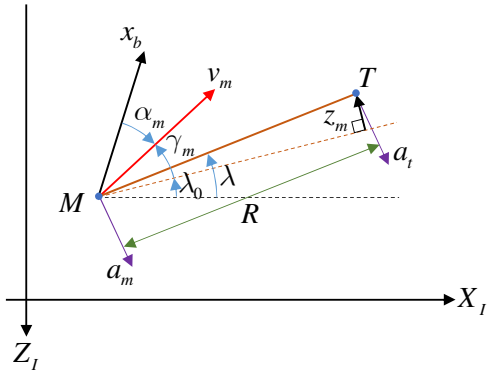

Fig. 3. Planar Engagement Geometry

In Fig. 3, $X_I - Z_I$ is an inertial coordinate system whose origin is located at the missile's initial centre of gravity. It is assumed that the missile is close to a collision course at the beginning of homing, and

the deviations are small enough during the homing phase so that linearisation around the initial Line-Of-Sight (LOS) with the angle of λ_0 is justifiable. Also, constant speed is assumed for both missile and target. x_b is a body-fixed coordinate system, and z_m is the relative displacement measured in the direction perpendicular to the initial LOS. R and λ are range and LOS angle, respectively. Furthermore, v_m, α_m, and γ_m are the speed, the angle of attack, and the flight path angle of the missile, respectively. a_m and a_t are accelerations of the missile and the target, respectively, in the direction perpendicular to the LOS. Note that the gravitational force is neglected in the engagement kinematics and a_t is assumed to be zero.

The missile motion in the homing phase is governed by i) the linearised kinematics, ii) the short-period mode longitudinal dynamics, and iii) the actuator dynamics represented by a first-order lag model. The system equation can be expressed as

$$\underbrace{\begin{bmatrix}\dot{\delta}_m\\ \dot{\alpha}_m\\ \dot{q}_m\\ \dot{\gamma}_m\\ \dot{z}_m\end{bmatrix}}_{\dot{\mathbf{x}}} = \underbrace{\begin{bmatrix}-\omega_a & 0 & 0 & 0 & 0\\ Z_\delta & Z_\alpha & 1 & 0 & 0\\ M_\delta & M_\alpha & M_q & 0 & 0\\ -Z_\delta & -Z_\alpha & 0 & 0 & 0\\ 0 & 0 & 0 & -v_m & 0\end{bmatrix}}_{\mathbf{A}} \underbrace{\begin{bmatrix}\delta_m\\ \alpha_m\\ q_m\\ \gamma_m\\ z_m\end{bmatrix}}_{\mathbf{x}} + \underbrace{\begin{bmatrix}\omega_a\\ 0\\ 0\\ 0\\ 0\end{bmatrix}}_{\mathbf{B}} \underbrace{\delta_c}_{\mathbf{u}} \tag{37}$$

$$a_m = v_m(\dot{\alpha}_m - q_m) = v_m Z_\alpha \alpha_m + v_m Z_\delta \delta_m$$

where δ_m is the fin deflection angle, δ_c is the fin deflection command, q_m is the pitch rate. Z_α, Z_δ, M_α, M_q, and M_δ denote the dimensional derivatives of the missile airframe, and ω_a is the cutoff frequency of the actuator. Parameter values used in the numerical simulation are borrowed from [39], [47] and are listed in Table III. The total engagement time is 2.0s, which corresponds to the initial range of 2000m, and the step size for numerical integration is 0.001s. Also, the initial LOS angle λ_0 is $0\,\mathrm{deg}$, and the target speed v_t is set to $500\mathrm{m/s}$. The initial state of the missile is set to $\mathbf{x}(t_0) = \begin{bmatrix}0\,\mathrm{deg} & 0\,\mathrm{deg} & 0\,\mathrm{deg/s} & -3\,\mathrm{deg} & 30\mathrm{m}\end{bmatrix}^T$.

TABLE III
PARAMETERS OF MISSILE DYNAMIC MODEL

Z_α	$-2.9399\mathrm{s}^{-1}$	Z_δ	$-0.6497\mathrm{s}^{-1}$
M_α	$-623.6149\mathrm{s}^{-2}$	M_q	$-5\mathrm{s}^{-1}$
M_δ	$-554.4808\mathrm{s}^{-2}$	ω_a	$100\mathrm{s}^{-1}$
v_m	$500\mathrm{m/s}$		

The simulation example considers an impact-angle-constrained interception problem which demands nullification of miss distance as well as achievement of the desired impact angle of $10\,\mathrm{deg}$. The multi-

variate constraints are described with the following matrices:

$$\mathbf{E} = \begin{bmatrix} 0 & 0 & 0 & 0 & 1 \\ 0 & 0 & 0 & 1 & 0 \end{bmatrix}, \quad \mathbf{z}_{f_d} = \begin{bmatrix} 0 \\ \pi/18 \end{bmatrix} \tag{38}$$

The formulation of this study differs from those of previous studies including [42], [45] in two aspects; i) this study explicitly considers the equality constraints whereas the previous studies dealt with minimisation without hard constraints, ii) the control law is derived considering the continuous-time formulation whereas the previous study of [45] considered the discrete-time dynamics.

C. Numerical Simulation

The primary objectives of the numerical simulation are twofold. The first is to verify that the control parametrisation method provides a feedback control law satisfying the given constraint, and the second is to demonstrate the process of trajectory shaping through modification of basis functions.

In the control parametrisation approach, the designer should decide not only the type but also the number of basis functions. One should choose which of the available feedback gain design formulae to use before proceeding to the designation of basis functions and solving for the coefficients. The procedure developed for the determined case in Sec. II-C is utilised in the following example.

1) Trial 1. Polynomial Basis: The first trial is to take the polynomial of t_{go} given by

$$\mathbf{\Psi}_1(t) = \begin{bmatrix} {t_{go}}^{n_1} \\ {t_{go}}^{n_2} \end{bmatrix} \tag{39}$$

as the basis function with the parameters satisfying $0 < n_1 < n_2$ so that the control input vanishes at the end. Parameter combinations $(n_1, n_2) = (1, 2)$ and $(2, 3)$ are considered for comparison.

Figure 5 shows the time responses of state variables and acceleration. Figures 5d and 5e show that γ_m and z_m converge to their target values at the final time for both pairs of polynomial degrees tested. Although δ_m, α_m, and q_m are not directly subject to the hard terminal constraint, these variables end up nearly nullified since the control input given by polynomials of t_{go} gradually vanishes as t approaches t_f. The rate of convergence in γ_m is faster with higher polynomial degrees. However, the shorter settling time comes at the cost of larger fin deflection and lateral acceleration as shown in Figs. 5a and 5f, respectively, which is also a consequence of using polynomial basis. More seriously, excessive overshoot can be witnessed in α_m, q_m, and a_m. Severe oscillation in the short-period mode variables should be avoided near the end of engagement to prevent any instabilities that may end in mission failure. In these regards, the first trial with simple polynomial basis functions turns out unsatisfactory.

2) Trial 2. Polynomial-Activation Basis: The basis function can be revised by incorporating the lessons provided by the previous trial. Polynomial of t_{go} is still valid as a prior for further refinement, as it has the advantages in nullifying the command at t_f and providing the degrees (n_1, n_2) as tunable parameters for adjusting the convergence rate. Results of Trial 1 suggest that the controller should avoid producing large initial commands to improve the transients. Accordingly, the revised choice is to incorporate an activation function f_{act} that performs smoothed initiation as follows:

$$\mathbf{\Psi}_2(t) = \mathbf{\Psi}_1(t) f_{\text{act}}\left(\frac{t_{go}}{t_f}\right) = \begin{bmatrix} {t_{go}}^{n_1} \\ {t_{go}}^{n_2} \end{bmatrix} f_{\text{act}}\left(\frac{t_{go}}{t_f}\right) \tag{40}$$

The activation function f_{act} should be similar to a sigmoid such that i) $f_{\text{act}}(t = t_f) = 1$ to preserve the characteristics of polynomial basis near the final time, ii) $f_{\text{act}}(t = 0) = 0$ so that the oscillatory response can be suppressed. Considering these two directions, f_{act} can be designed as follows:

$$f_{\text{act}}\left(\frac{t_{go}}{t_f}\right) = \text{sech}\left[k\left(\frac{t_{go}}{t_f}\right)^m\right] \tag{41}$$

where $k > 0$ and $m > 0$ are design parameters. Transition from 1 to 0 as $t_{go} \to t_f$ becomes steeper as m increases. Also, transition from 1 to 0 begins at a smaller t_{go}/t_f with increased k. Let us define $R_{1/2}$ as the point of half-activation, that is,

$$f_{\text{act}}\left(R_{1/2}\right) = 0.5 \tag{42}$$

The point $R_{1/2}$ can be regarded as the parameter determining the centre of control activation. To this end, one may solve for the corresponding k by substituting Eq. (42) into Eq. (41) as

$$k = \frac{\text{sech}^{-1}(0.5)}{{R_{1/2}}^m} \tag{43}$$

Figure 4a shows the activation function with varied $R_{1/2}$, and Fig. 4b shows the corresponding basis function of the form $\Psi(t) = {t_{go}}^n f_{\text{act}}\left(\frac{t_{go}}{t_f}\right)$ with normalisation, while m is fixed to be 5. Figures 4a and 4b show that decreasing $R_{1/2}$ delays the activation, i.e., transition from 0 to 1.

Substituting Eqs. (41) and (43) into Eq. (40) yields the final form of the basis function considered in Trial 2 as

$$\mathbf{\Psi}_2(t) = \begin{bmatrix} {t_{go}}^{n_1} \\ {t_{go}}^{n_2} \end{bmatrix} \text{sech}\left[\text{sech}^{-1}(0.5)\left(\frac{t_{go}/t_f}{R_{1/2}}\right)^m\right] \tag{44}$$

Here, n_1, n_2, and $R_{1/2}$ are considered as tunable design parameters while m is set to a fixed value 5 for simplicity. The design parameter combinations are sought from $n_1, n_2 \in \{1, 2, 3, 4\}$ and $R_{1/2} \in \{0.4, 0.5, 0.6, 0.7, 0.8, 0.9\}$. Parametric study is performed to find the best combination for two different shaping objectives.

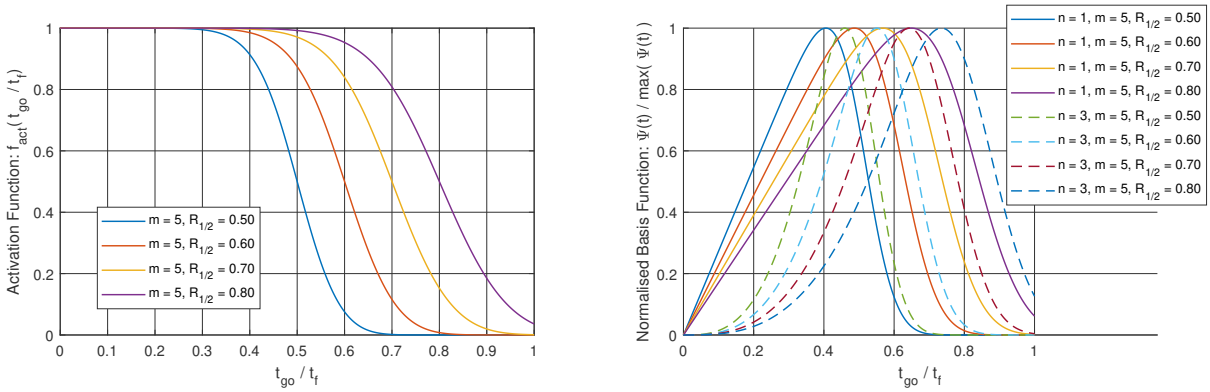

(a) Activation Function

(b) Corresponding Basis Function

Fig. 4. Basis Function Candidates for Trial 2

The first objective is to minimise the maximum absolute value of pitch rate in the entire engagement.

$$\text{minimise} \quad J_1 = \max_{t\in[t_0,t_f]} |q_m(t)| \tag{45}$$

The combination $\left(n_1, n_2, R_{1/2}\right) = (1,\, 2,\, 0.8)$ exhibited the best characteristics as assessed by J_1. As shown in Figs. 5d and 5e, the corresponding control law shows good performance in achieving terminal output constraints. The oscillatory transients are barely observed in the responses of α_m, q_m, and a_m. The pitch rate response shows an acceptable level of peak value. Therefore, the command and trajectory profiles obtained by minimising J_1 are satisfactory.

The second objective is to emphasise suppression of α_m, q_m, and a_m in both the beginning and the end of engagement.

$$\text{minimise} \quad J_2 = \sum_{t\in\mathbf{T}_1} {a_m}^2\,(t) + r_0 \max_{t\in\mathbf{T}_2} |a_m\,(t)| \tag{46}$$

In Eq. (46), $r_0 = 0.5$, $\mathbf{T}_1 = [t_0, t_0 + 0.05] \cup [t_f - 0.05, t_f]$, and $\mathbf{T}_2 = [t_0, t_f]$. The search for the parameters returned $\left(n_1, n_2, R_{1/2}\right) = (2,\, 3,\, 0.7)$ as the best compromise with respect to J_2. In addition to satisfying the terminal constraints imposed on z_m and γ_m, the responses of α_m, q_m and a_m are insignificant in the initial period by virtue of reduced δ_m as well as in the final region. Consequently, the control effort is concentrated in the middle of engagement as shown in Figs. 5a and 5f.

Contrary to Trial 1, the oscillatory fluctuations in α_m, q_m, and a_m are reduced in Trial 2. The activation function introduced in the basis function prevents excitation of short-period mode due to large initial control demand since the command δ_c begins with 0. Instead, it delays the point of maximum control surface deflection. Nevertheless, δ_c converges to 0 as $t \to t_f$ at the rate determined by the polynomial degrees. If $n_1, n_2 \geq 2$, then $\dot{\delta}_c$ also tends to 0 as $t \to t_f$ which is beneficial for allowing a period of time to maintain $\delta_c \approx 0$ around t_f, resulting in enough control authority and passive nullification of

α_m. Also, the case with greater values for (n_1, n_2) reaches a larger maximum acceleration than the case with smaller values as shown in Fig. 5f. The difference between peak accelerations is smaller in Trial 2 than in Trial 1, which indicates reduced influence of the polynomial term in the basis functions due to employing the activation function.

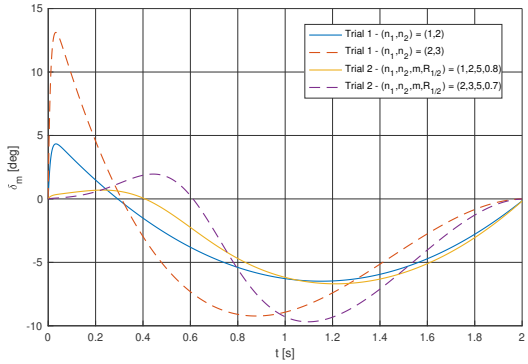

(a) Control Surface Deflection Angle

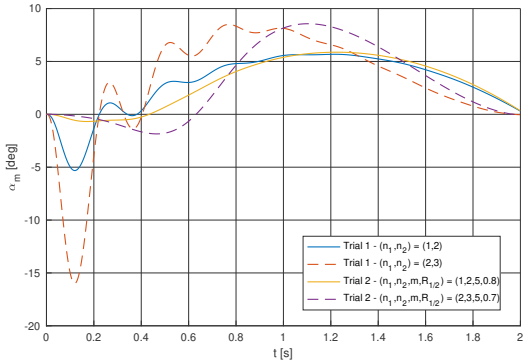

(b) Angle of Attack

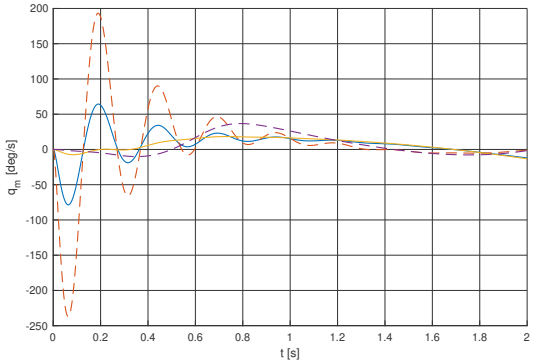

(c) Pitch Rate

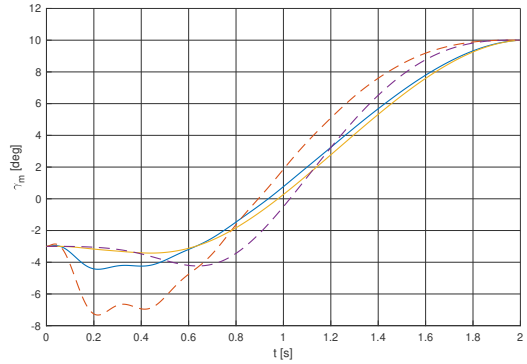

(d) Flight Path Angle

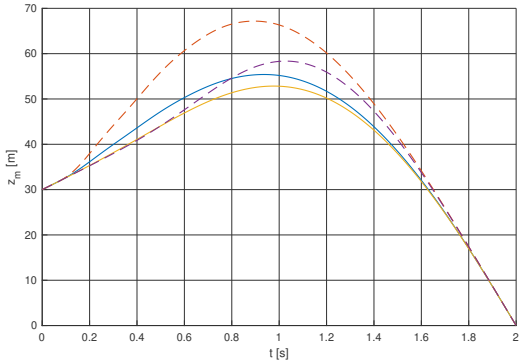

(e) Relative Displacement Between Missile and Target

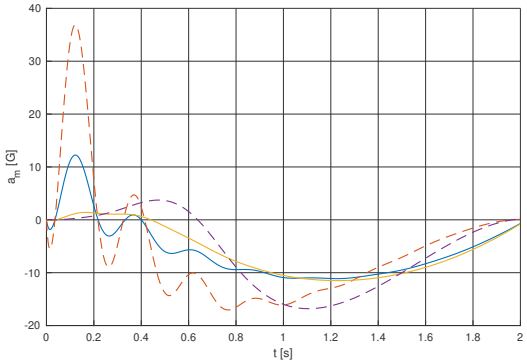

(f) Lateral Acceleration

Fig. 5. Time Histories of Missile State Variables

In summary, the process of constructing the basis functions shows how an appropriate feedback controller can be synthesised to satisfy the given terminal output constraint by using the notion of control parametrisation. Trajectory shaping can be performed more directly in this approach, for example, by sequential modification of the basis functions. After specifying the form of basis functions, one can choose the basis parameters either by combinatorial search or by optimisation considering detailed tuning goals.

V. Conclusions

This study presented the control parametrisation method for terminal control problems where trajectory shaping is of concern. The principle is similar in its essence to interpolating the current point and the desired final point with a curve, in that the coefficients are determined to satisfy given boundary conditions with the basis functions chosen a priori. Parametric structure for the control input allows tuning interfaces through the wide variety of linearly independent basis functions. In turn, control parametrisation can be seen as an alternative that complements linear quadratic optimal control.

Usefulness of the proposed method was demonstrated with missile guidance applications. This study revisited trajectory shaping guidance laws from the control parametrisation perspective by characterising the associated basis functions. Also, the application example considering integrated guidance and control demonstrated the design procedure centred around construction of appropriate basis functions. The simulation results showed that the resulting finite-horizon controllers satisfy given terminal constraints while the closed-loop trajectory can be shaped as intended.

Appendix A
Invariance of Coefficient Along Trajectory

Suppose that $\mathbf{k}_0$ is obtained for the trajectory starting from $\mathbf{x}(t_0)$ predicted at t_0 to satisfy the given constraint, that is,

$$\mathbf{E}\left[\mathbf{F}(t_f,t_0)\,\mathbf{k}_0+\mathbf{\Phi}(t_f,t_0)\,\mathbf{x}(t_0)+\mathbf{f}(t_f,t_0)\right]=\mathbf{z}_{f_d} \tag{47}$$

Likewise, suppose that $\mathbf{k}$ is obtained for the trajectory starting from $\mathbf{x}(t)$ predicted at t to satisfy the given constraint as

$$\mathbf{E}\left[\mathbf{F}(t_f,t)\,\mathbf{k}+\mathbf{\Phi}(t_f,t)\,\mathbf{x}(t)+\mathbf{f}(t_f,t)\right]=\mathbf{z}_{f_d} \tag{48}$$

If $\mathbf{x}(t)$ in Eq. (48) is on the trajectory that starts from $\mathbf{x}(t_0)$ and evolves along the dynamics with the control law solved for t_0 in the absence of uncertainty, $\mathbf{x}(t)$ can be represented as

$$\mathbf{x}(t)=\mathbf{F}(t,t_0)\,\mathbf{k}_0+\mathbf{\Phi}(t,t_0)\,\mathbf{x}(t_0)+\mathbf{f}(t,t_0) \tag{49}$$

Substituting Eq. (49) into Eq. (48), we have

$$\mathbf{E}\left[\mathbf{F}\left(t_f,t\right)\mathbf{k}+\mathbf{\Phi}\left(t_f,t\right)\mathbf{F}\left(t,t_0\right)\mathbf{k}_0+\mathbf{\Phi}\left(t_f,t_0\right)\mathbf{x}\left(t_0\right)+\mathbf{\Phi}\left(t_f,t\right)\mathbf{f}\left(t,t_0\right)+\mathbf{f}\left(t_f,t\right)\right]=\mathbf{z}_{f_d} \tag{50}$$

Because $\mathbf{\Phi}\left(t_f,t\right)\mathbf{F}\left(t,t_0\right)+\mathbf{F}\left(t_f,t\right)=\mathbf{F}\left(t_f,t_0\right)$ and $\mathbf{\Phi}\left(t_f,t\right)\mathbf{f}\left(t,t_0\right)+\mathbf{f}\left(t_f,t\right)=\mathbf{f}\left(t_f,t_0\right)$, Eq. (50) can be rewritten as

$$\mathbf{E}\left[\mathbf{F}\left(t_f,t\right)\mathbf{k}+\left\{\mathbf{F}\left(t_f,t_0\right)-\mathbf{F}\left(t_f,t\right)\right\}\mathbf{k}_0+\mathbf{\Phi}\left(t_f,t_0\right)\mathbf{x}\left(t_0\right)+\mathbf{f}\left(t_f,t_0\right)\right]=\mathbf{z}_{f_d} \tag{51}$$

Equating Eq. (47) and Eq. (51) yields $\mathbf{EF}\left(t_f,t\right)\left(\mathbf{k}-\mathbf{k}_0\right)=\mathbf{0}$ which shows that $\mathbf{k}=\mathbf{k}_0$ should hold for any t as long as $\mathbf{x}\left(t\right)$ is on the trajectory described by Eq. (49). This indicates invariance of the coefficient $\mathbf{k}$ along the ideal trajectory assuming that $\mathbf{EF}\left(t_f,t\right)$ is invertible, $\forall t\in\left[t_0,t_f\right)$. This confirms that open-loop and closed-loop implementations are equivalent in the ideal dynamics.

APPENDIX B
QUADRATIC PROGRAMMING FOR UNDERDETERMINED CASE

The optimality conditions pertaining to the problem in Eq. (17) are the primal and dual feasibility equations that together form the Karush-Kuhn-Tucker (KKT) system as

$$\begin{bmatrix}\mathbf{G}\left(t\right) & \left\{\mathbf{EF}\left(t_f,t\right)\right\}^T\\ \mathbf{EF}\left(t_f,t\right) & \mathbf{0}\end{bmatrix}\begin{bmatrix}\mathbf{k}^*\\ \boldsymbol{\lambda}^*\end{bmatrix}=\begin{bmatrix}-\mathbf{g}\left(t\right)\\ \mathbf{z}_{f_d}-\mathbf{E\Phi}\left(t_f,t\right)\mathbf{x}\left(t\right)-\mathbf{Ef}\left(t_f,t\right)\end{bmatrix} \tag{52}$$

The behaviour of the solution set for the KKT system is well-understood [48]. A unique optimal solution exists if the KKT matrix in Eq. (52) is nonsingular. If the KKT matrix is singular while the KKT system is solvable, any feasible solution provides an optimal pair. However, if the KKT system is not solvable, then the QP problem is unbounded below.

The state-of-the-art convex optimisation algorithms such as the interior-point method [4] can solve the QP problem in Eq. (17) efficiently. However, computational overhead during a short control update period should not be excessive, therefore, the philosophy similar to explicit model predictive control is preferred. The approach avoiding online optimisation is to pre-calculate the gain matrices and store them as time-to-go-indexed tables for later use in online evaluation of the control law.

Analytical solution can be obtained if the QP problem is well-posed. Assuming that $\mathbf{G}\left(t\right)>0$, $\mathbf{G}\left(t\right)$ is nonsingular, Eq. (52) can be solved for $\mathbf{k}^*$ as

$$\mathbf{k}^*=-\mathbf{G}^{-1}\left(t\right)\left[\mathbf{g}\left(t\right)+\left\{\mathbf{EF}\left(t_f,t\right)\right\}^T\boldsymbol{\lambda}^*\right] \tag{53}$$

Substituting Eq. (53) into Eq. (52) leads to

$$-\mathbf{EF}\left(t_f,t\right)\mathbf{G}^{-1}\left(t\right)\left[\mathbf{g}\left(t\right)+\left\{\mathbf{EF}\left(t_f,t\right)\right\}^T\boldsymbol{\lambda}^*\right]=\mathbf{z}_{f_d}-\mathbf{E\Phi}\left(t_f,t\right)\mathbf{x}\left(t\right)-\mathbf{Ef}\left(t_f,t\right) \tag{54}$$

If $\mathbf{\Psi}(t)$ is chosen so that $\mathbf{EF}(t_f,t)$ is full (row) rank, $\mathbf{EF}(t_f,t)\,\mathbf{G}(t)\,\{\mathbf{EF}(t_f,t)\}^T > 0$, Eq. (54) can be solved for $\boldsymbol{\lambda}^*$ as

$$\begin{aligned}\boldsymbol{\lambda}^* = &-\left[\mathbf{EF}(t_f,t)\,\mathbf{G}^{-1}(t)\,\{\mathbf{EF}(t_f,t)\}^T\right]^{-1}\\ &\times\left\{\mathbf{EF}(t_f,t)\,\mathbf{G}^{-1}(t)\,\mathbf{g}(t)+\mathbf{z}_{f_d}-\mathbf{E\Phi}(t_f,t)\,\mathbf{x}(t)-\mathbf{Ef}(t_f,t)\right\}\end{aligned} \tag{55}$$

Note that $\mathbf{F}(t_f,t)\in\mathbb{R}^{n\times q}$ being a matrix of rank n together with $\mathbf{E}\in\mathbb{R}^{p\times n}$ being full rank as described in Sec. II-A is a strong sufficient condition for $\mathbf{EF}(t_f,t)\in\mathbb{R}^{p\times q}$ being full rank, because $\operatorname{rank}(\mathbf{EF}(t_f,t)) = \operatorname{rank}(\mathbf{E}) = p < q$ under this condition. The optimal coefficient $\mathbf{k}^*$ can be derived by substituting Eq. (55) again into Eq. (53) as

$$\begin{aligned}\mathbf{k}^* = -\mathbf{G}^{-1}(t)\Big[&\mathbf{g}(t)-\{\mathbf{EF}(t_f,t)\}^T\left[\mathbf{EF}(t_f,t)\,\mathbf{G}^{-1}(t)\,\{\mathbf{EF}(t_f,t)\}^T\right]^{-1}\\ &\times\left\{\mathbf{EF}(t_f,t)\,\mathbf{G}^{-1}(t)\,\mathbf{g}(t)+\mathbf{z}_{f_d}-\mathbf{E\Phi}(t_f,t)\,\mathbf{x}(t)-\mathbf{Ef}(t_f,t)\right\}\Big]\end{aligned} \tag{56}$$

Finally, substitution of Eq. (56) into Eq. (3) gives the control law as shown in Eqs. (19) and (20).

REFERENCES

[1] J.-N. Juang, J. D. Turner, and H. M. Chun, "Closed-Form Recursive Formula for an Optimal Tracker with Terminal Constraints," *Journal of Optimization Theory and Applications*, vol. 51, no. 2, pp. 307–320, 1986.

[2] L. Ntogramatzidis, "A Simple Solution to the Finite-Horizon LQ Problem with Zero Terminal State," *Kybernetika*, vol. 39, no. 4, pp. 483–492, 2003.

[3] A. Ferrante and L. Ntogramatzidis, "A Unified Approach to the Finite-Horizon Linear Quadratic Optimal Control Problem," *European Journal of Control*, vol. 13, no. 5, pp. 473–488, 2007.

[4] M. Grant and S. Boyd, "Graph Implementations for Nonsmooth Convex Programs," *Recent Advances in Learning and Control*, V. Blondel, S. Boyd, and H. Kimura, Eds. London, UK: Springer, 2008, pp. 95–110.

[5] A. Zanelli, A. Domahidi, J. Jerez, and M. Morari, "FORCES NLP: an Efficient Implementation of Interior-Point Methods for Multistage Nonlinear Nonconvex Programs," *International Journal of Control*, vol. 93, no. 1, pp. 13–29, 2020.

[6] X. Liu, P. Lu, and B. Pan, "Survey of Convex Optimization for Aerospace Applications," *Astrodynamics*, vol. 1, no. 1, pp. 23–40, 2017.

[7] Y. Mao, M. Szmuk, and B. Açikmeşe, "A Tutorial on Real-time Convex Optimization Based Guidance and Control for Aerospace Applications," *American Control Conference*, Milwaukee, WI, June 2018.

[8] H. R. Sirisena and F. S. Chou, "Convergence of the Control Parametrization Ritz Method for Nonlinear Optimal Control Problems," *Journal of Optimization Theory and Applications*, vol. 29, no. 3, pp. 369–382, 1979.

[9] C. J. Goh and K. L. Teo, "Control Parametrization: a Unified Approach to Optimal Control Problems with General Constraints," *Automatica*, vol. 24, no. 1, pp. 3–18, 1988.

[10] K. L. Teo, L. S. Jennings, H. W. J. Lee, and V. Rehbock, "The Control Parametrization Enhancing Transform for Constrained Optimal Control Problems," *Journal of the Australian Mathematical Society, Series B, Applied Mathematics*, vol. 40, no. 3, pp. 314–335, 1999.

[11] Q. Lin, R. Loxton, and K. L. Teo, "The Control Parameterization Method for Nonlinear Optimal Control: A Survey," *Journal of Industrial and Management Optimization*, vol. 10, no. 1, pp. 275–309, 2014.

[12] N. Cho, Y. Kim, and H.-S. Shin, "Generalization of Linearly Parametrized Trajectory Shaping Guidance Laws," *20th IFAC World Congress*, Toulouse, France, July 2017.

[13] E. Kreindler, "Optimality of Proportional Navigation," *AIAA Journal*, vol. 11, no. 6, pp. 878–880, 1973.

[14] G. W. Cherry, "A General, Explicit, Optimizing Guidance Law for Rocket-Propelled Spaceflight," *Astrodynamics Guidance and Control Conference*, Los Angeles, CA, USA, August 1964.

[15] C.-K. Ryoo, H. Cho, and M.-J. Tahk, "Time-to-Go Weighted Optimal Guidance with Impact Angle Constraints," *IEEE Transactions on Control Systems Technology*, vol. 14, no. 3, pp. 483–492, 2006.

[16] J.-I. Lee, I.-S. Jeon, and C.-H. Lee, "Command-Shaping Guidance Law Based on a Gaussian Weighting Function," *IEEE Transactions on Aerospace and Electronic Systems*, vol. 50, no. 1, pp. 772–777, 2014.

[17] C.-H. Lee, T.-H. Kim, M.-J. Tahk, and I.-H. Whang, "Polynomial Guidance Laws Considering Terminal Impact Angle and Acceleration Constraints," *IEEE Transactions on Aerospace and Electronic Systems*, vol. 49, no. 1, pp. 74–92, 2013.

[18] H.-S. Shin, J.-I. Lee, and M.-J. Tahk, "A New Homing Guidance Law to Reduce Sensitivity on Initial Heading Errors," *Proceedings of the Institution of Mechanical Engineers, Part G: Journal of Aerospace Engineering*, vol. 229, no. 9, pp. 1740–1753, 2015.

[19] V. Shaferman and T. Shima, "Linear Quadratic Guidance Laws for Imposing a Terminal Intercept Angle," *Journal of Guidance, Control, and Dynamics*, vol. 31, no. 5, pp. 1400–1412, 2008.

[20] N. Cho and Y. Kim, "Optimality of Augmented Ideal Proportional Navigation for Maneuvering Target Interception," *IEEE Transactions on Aerospace and Electronic Systems*, vol. 52, no. 2, pp. 948–954, 2016.

[21] D. Alkaher, A. Moshaiov, and Y. Or, "Guidance Laws Based on Optimal Feedback Linearization Pseudocontrol with Time-to-Go Estimation," *Journal of Guidance, Control, and Dynamics*, vol. 37, no. 4, pp. 1298–1305, 2014.

[22] C.-K. Ryoo, H. Cho, and M.-J. Tahk, "Optimal Guidance Laws with Terminal Impact Angle Constraint," *Journal of Guidance, Control, and Dynamics*, vol. 28, no. 4, pp. 724–732, 2005.

[23] I.-S. Jeon and J.-I. Lee, "Optimality of Proportional Navigation Based on Nonlinear Formulation," *IEEE Transactions on Aerospace and Electronic Systems*, vol. 46, no. 4, pp. 2051–2055, 2010.

[24] A. Ratnoo and D. Ghose, "Impact Angle Constrained Interception of Stationary Targets," *Journal of Guidance, Control, and Dynamics*, vol. 31, no. 6, pp. 1817–1822, 2008.

[25] ——, "Impact Angle Constrained Guidance Against Nonstationary Nonmaneuvering Targets," *Journal of Guidance, Control, and Dynamics*, vol. 33, no. 1, pp. 269–275, 2010.

[26] S. Ghosh, O. A. Yakimenko, D. T. Davis, and T. H. Chung, "Unmanned Aerial Vehicle Guidance for an All-Aspect Approach to a Stationary Point," *Journal of Guidance, Control, and Dynamics*, vol. 40, no. 11, pp. 2871–2888, 2017.

[27] Y.-I. Lee, S.-H. Kim, and M.-J. Tahk, "Optimality of Linear Time-Varying Guidance for Impact Angle Control," *IEEE Transactions on Aerospace and Electronic Systems*, vol. 48, no. 4, pp. 2802–2817, 2012.

[28] E. J. Ohlmeyer and C. A. Phillips, "Generalized Vector Explicit Guidance," *Journal of Guidance, Control, and Dynamics*, vol. 29, no. 2, pp. 261–268, 2006.

[29] P. Lu, "Theory of Fractional-Polynomial Powered Descent Guidance," *Journal of Guidance, Control, and Dynamics*, vol. 43, no. 3, pp. 398–409, 2020.

[30] C.-H. Lee, M.-J. Tahk, and J.-I. Lee, "Generalized Formulation of Weighted Optimal Guidance Laws with Impact Angle Constraint," *IEEE Transactions on Aerospace and Electronic Systems*, vol. 49, no. 2, pp. 1317–1322, 2013.

[31] J. Z. Ben-Asher and S. Levinson, "New Proportional Navigation Law for Ground-to-Air Systems," *Journal of Guidance, Control, and Dynamics*, vol. 26, no. 5, pp. 822–825, 2003.

[32] M.-Y. Ryu, C.-H. Lee, and M.-J. Tahk, "Command Shaping Optimal Guidance Laws against High-Speed Incoming Targets," *Journal of Guidance, Control, and Dynamics*, vol. 38, no. 10, pp. 2025–2033, 2015.

[33] C.-H. Lee, "Optimal Guidance Laws Using Generalized Weighting Functions," Ph.D. dissertation, Department of Aerospace Engineering, Korea Advanced Institute of Science and Technology, Korea, 2013.

[34] A. E. Bryson Jr., "Linear Feedback Solutions for Minimum Effort Interception, Rendezvous, and Soft Landing," *AIAA Journal*, vol. 3, no. 8, pp. 1542–1544, 1965.

[35] A. R. Klumpp, "Apollo Lunar Descent Guidance," *Automatica*, vol. 10, no. 2, pp. 133–146, 1974.

[36] P. Lu, "Augmented Apollo Powered Descent Guidance," *Journal of Guidance, Control, and Dynamics*, vol. 42, no. 3, pp. 447–457, 2019.

[37] C.-H. Lee, J.-I. Lee, and M.-J. Tahk, "Sinusoidal Function Weighted Optimal Guidance Laws," *Proceedings of the Institution of Mechanical Engineers, Part G: Journal of Aerospace Engineering*, vol. 229, no. 3, pp. 534–542, 2015.

[38] C.-H. Lee, T.-H. Kim, and M.-J. Tahk, "Interception Angle Control Guidance Using Proportional Navigation with Error Feedback," *Journal of Guidance, Control, and Dynamics*, vol. 36, no. 5, pp. 1556–1561, 2013.

[39] T. Shima, M. Idan, and O. M. Golan, "Sliding-Mode Control for Integrated Missile Autopilot Guidance," *Journal of Guidance, Control, and Dynamics*, vol. 29, no. 2, pp. 250–260, 2006.

[40] S. S. Vaddi, P. K. Menon, and E. J. Ohlmeyer, "Numerical State-Dependent Riccati Equation Approach for Missile Integrated Guidance Control," *Journal of Guidance, Control, and Dynamics*, vol. 32, no. 2, pp. 699–703, 2009.

[41] Y. B. Shtessel and C. H. Tournes, "Integrated Higher-Order Sliding Mode Guidance and Autopilot for Dual-Control Missiles," *Journal of Guidance, Control, and Dynamics*, vol. 32, no. 1, pp. 79–94, 2009.

[42] M. Levy, T. Shima, and S. Gutman, "Linear Quadratic Integrated Versus Separated Autopilot-Guidance Design," *Journal of Guidance, Control, and Dynamics*, vol. 36, no. 6, pp. 1722–1730, 2013.

[43] R. Padhi, C. Chawla, and P. G. Das, "Partial Integrated Guidance and Control of Interceptors for High-Speed Ballistic Targets," *Journal of Guidance, Control, and Dynamics*, vol. 37, no. 1, pp. 149–163, 2014.

[44] X. Wang and J. Wang, "Partial Integrated Guidance and Control with Impact Angle Constraints," *Journal of Guidance, Control, and Dynamics*, vol. 38, no. 5, pp. 925–936, 2015.

[45] J.-H. Kim, I. H. Whang, and B. M. Kim, "Finite Horizon Integrated Guidance and Control for Terminal Homing in Vertical Plane," *Journal of Guidance, Control, and Dynamics*, vol. 39, no. 5, pp. 1104–1112, 2016.

[46] V. Bachtiar, C. Manzie, and E. C. Kerrigan, "Nonlinear Model-Predictive Integrated Missile Control and Its Multiobjective Tuning," *Journal of Guidance, Control, and Dynamics*, vol. 40, no. 11, pp. 2961–2970, 2017.

[47] P. Zarchan, *Tactical and Strategic Missile Guidance*. Reston, VA: American Institute of Aeronautics and Astronautics, 2012, pp. 473–527.

[48] S. Boyd and L. Vandenberghe, *Convex Optimization*. Cambridge, United Kingdom: Cambridge University Press, 2004, pp. 521–560.

Namhoon Cho (M'16) received the B.S. and Ph.D. degrees in Mechanical and Aerospace Engineering from Seoul National University, the Republic of Korea, in 2012 and 2017, respectively. He is currently a research fellow in the Centre for Autonomous and Cyber-Physical Systems, Cranfield University, United Kingdom, since 2021. Previously, he was a senior researcher in the Agency for Defense Development, the Republic of Korea, between 2019 and 2020, working on research and development of guidance and control systems. He was a research fellow in the Department of Mechanical and Aerospace Engineering, Seoul National University, between 2017 and 2019. His current research interests include robust adaptive control based on online model learning, machine learning applications for flight control, unified frameworks for automated design of optimal guidance and control systems, Bayesian approaches to stochastic optimal control, and trajectory optimisation.

Jongho Park received his B.S., M.S., and Ph.D. degrees in aerospace engineering from the Department of Mechanical and Aerospace Engineering, Seoul National University, Seoul, Republic of Korea, in 2010, 2012, and 2016, respectively. From 2016 to 2019, he was a Senior Researcher for Guidance and Control team in Agency for Defense Development, Daejeon, Republic of Korea. He joined the faculty of Ajou University in 2019, where he is currently an Assistant Professor in the Department of Military Digital Convergence. His current research interests include guidance, control, and application of aerospace systems.

Youdan Kim (M'94–SM'16) received the B.S. and M.S. degrees in Aeronautical Engineering from Seoul National University, the Republic of Korea, in 1983 and 1985, respectively, and a Ph.D. in Aerospace Engineering from Texas A&M University in 1990. He joined the Faculty of Seoul National University in 1992, where he is currently a professor at the Department of Aerospace Engineering. His current research interests include nonlinear flight control, reconfigurable control, path planning, and guidance techniques for aerospace applications.

Hyo-Sang Shin received his BSc from Pusan National University in 2004 and gained an MSc on flight dynamics, guidance and control in Aerospace Engineering from KAIST and a PhD on cooperative missile guidance from Cranfield University in 2006 and 2010, respectively. He is currently a Professor of Guidance, Control and Navigation (GNC) Systems in Autonomous and Intelligent Systems Group at Cranfield University. His current research interests include target tracking, adaptive and sensor-based control, data-centric GNC, and distributed control of multiple agent systems.

https://dspace.org/

Unified control parameterization approach for finite-horizon feedback control with trajectory shaping

Cho, Namhoon; Park, Jongho; Kim, Youdan; Shin, Hyo-Sang

2022-03-22
Institute of Electrical and Electronics Engineers (IEEE)
https://doi.org/10.1109/TAES.2022.3160990
Cho N, Park J, Kim Y, Shin H-S. (2022) Unified control parameterization approach for finite-horizon feedback control with trajectory shaping. IEEE Transactions on Aerospace and Electronic Systems, Volume 58, Issue 5, October 2022, pp. 4782-4795

Downloaded from a DSpace repository. https://dspace.org/